Characterization of Ketones Formed in the Open System Corrosion Test of Naphthenic Acids by Fourier Transform Ion Cyclotron Resonance Mass Spectrometry

Logan C. Krajewski,[†] Winston K. Robbins,[‡,§] Yuri E. Corilo,[∥] Gheorghe Bota,[§] Alan G. Marshall,*,[†,∥] and Ryan P. Rodgers[†,∥]

[†]Department of Chemistry and Biochemistry, Florida State University, 95 Chieftain Way, Tallahassee, Florida 32306, United States
[‡]Consultant, Future Fuels Institute and [∥]Ion Cyclotron Resonance Program, National High Magnetic Field Laboratory, Florida State University, 1800 East Paul Dirac Drive, Tallahassee, Florida 32310, United States
[§]Institute for Corrosion and Multiphase Technology, Ohio University, 342 West State Street, Athens, Ohio 45701, United States

Ⓢ *Supporting Information*

ABSTRACT: Because the rate of naphthenic acid corrosion does not correlate with the concentration of acids, it has been proposed that a subset of naphthenic acids in petroleum fractions may be more corrosive than others. The primary corrosion products (iron naphthenates) decompose to form ketones at corrosion temperatures (250−400 °C), so characterization of ketones in corrosion fluids could potentially be used to identify the reactive acids that generated the iron naphthenate. Previous work with model acids has reported the development of a method to characterize such ketones by isolation with strong anion exchange separation and detection, with the assistance of ketone targeting derivatization reagent, by Fourier transform ion cyclotron resonance mass spectrometry. Here, we extend that method to characterize the ketones formed in a corrosion test by use of commercially available naphthenic acids (NAP) in a flow-through reactor. The NAP corrosion test yields a single O_1 ketones/aldehydes distribution close to that predicted from the O_2 acids distribution before corrosion, with no bias in the carbon number and a slight bias toward lower double bond equivalents in the reactive acids detected. Ketone distributions did not appear to change over the 24 h test. With a fluid residence time of only ∼30 min at reactor temperature, the results suggest that the ketones were formed rapidly beneath an FeS scale.

■ INTRODUCTION

"Opportunity crudes" are available at lower prices due to higher concentrations of sulfur and naphthenic acids (carboxylic acids found in petroleum).[1] Both reactive sulfur (i.e., sulfur species that oxidize iron) and naphthenic acids cause corrosion in crude oil refineries, at a cost on the order of billions of dollars annually for the petroleum industry.[2] Reactive sulfur corrodes steel at high temperatures (230−400 °C) to form an insoluble iron sulfide scale, whereas naphthenic acids at the same temperatures react with steel to form oil-soluble iron naphthenates.[3] These corrosion processes, in the absence of water, may be summarized by three free radical reactions[4]

$$Fe_{(s)} + 2RCOOH \rightarrow Fe(RCOO)_2 + 2H^\bullet \quad (1)$$

$$Fe_{(s)} + H_2S \rightarrow FeS_{(s)} + 2H^\bullet \quad (2)$$

$$Fe(RCOO)_2 + H_2S \rightleftharpoons FeS_{(s)} + 2RCOOH \quad (3)$$
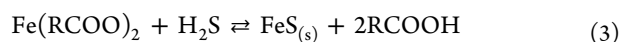
in which R represents the hydrocarbon portion of the reactive carboxylic acid and H_2S is used as surrogate for reactive sulfur. As indicated in reaction 3, in addition to direct reaction with the iron, H_2S (or other reactive S) can react with the iron naphthenate product and regenerate acids. It should be noted, however, that the reverse reaction may also occur (i.e., acids can react with the FeS scale), and it is often suggested that both reactions 1 & 2 may occur by solid-state diffusion of iron

through the scale. The FeS scale generated in reactions 2 and 3 has been shown to inhibit corrosion unpredictably due to differences in the acid/sulfur ratio and shear forces on refinery wall surfaces.[4−8]

In corrosion tests with vacuum gas oils, scales have been observed that contain not only FeS but also an insoluble iron oxide (magnetite) layer that appears to increase resistance against further corrosion.[5,9,10] When challenged by acid alone, magnetite appears to be generated underneath the previously existent scale.[11−13] Model acid studies have shown that the magnetite layer can be generated as a result of thermal decomposition of iron naphthenate (generated by reaction 1) in the oil[13,14]

$$Fe(RCOO)_2 \rightarrow FeO + CO_2 + RCOR \quad (4)$$

$$4FeO \rightarrow Fe_3O_4 + \alpha\text{-}Fe \quad (5)$$
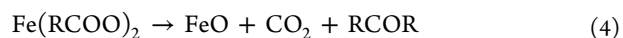
At temperatures greater than 250 °C, solution-phase thermal decomposition of iron naphthenates begins to generate carbon dioxide, wüstite (FeO), and a ketone (reaction 4).[15] The wüstite is thermodynamically unstable below ∼550 °C and disproportionates into ferrite (α-Fe) and magnetite (Fe_3O_4) (reaction 5).[16,17]

The naphthenic acid corrosion of iron (reaction 1) depends on the shape and size of the reactive carboxylic acids.[3] The distributions of naphthenic acids in crudes differ widely in shape and size due to variability in their geological origin.[18−20] Tens of thousands of naphthenic acids, with molecular weights (MW) that range between 200 and 1000 Da, have been characterized in a single drop of oil.[21,22] The compositional complexity and variability of naphthenic acids in petroleum play a role in the lack of a good correlation between their concentration and corrosivity. Generally, corrosion is considered to increase with naphthenic acid concentration,[23] as measured by the total acid number (TAN, the amount of potassium hydroxide in mg needed to neutralize 1 g of oil) and as acids approach their boiling point.[24,25] It is therefore postulated that a subset of the total naphthenic acids is primarily responsible for iron corrosion.[26,27] Thermal decomposition of iron naphthenates (reaction 4) would be expected to generate an oil-soluble ketone that retains the molecular composition and structure of the two acids that formed the iron naphthenate. Previously, we reported the development of a method that characterizes the ketones generated in corrosion tests with individual model acids.[28] That method combines a chromatographic separation and carbonyl-specific derivatization with detection by Fourier transform ion cyclotron resonance mass spectrometry (FT-ICR MS). A multistep procedure was required to separate corrosion-derived ketones from unreacted acid and other possible existing oxygen containing compounds (either pre-existing in the sample or formed during corrosion test) and confirmed that the O_1 molecular composition was truly that of a carbonyl compound. Here, the method has been applied to effluents from a corrosion test carried out with a commercially available naphthenic acid mixture (NAP). In the present test, iron oxide scales have been formed on the surface of metal samples with pre-existent sulfide scales. The objective of this work was to demonstrate the applicability of the method to a mixture of acids and to identify any selectivity in ketone formation.

■ EXPERIMENTAL METHODS

Materials. HPLC grade dichloromethane (DCM), toluene, and methanol were purchased from J.T. Baker Chemicals (Phillipsburg, PA) and used as received. Commercial naphthenic acids (TCI America, Portland, OR) were used, along with purchased white mineral oil (average MW, 530 Da) (Tufflo 6056, Calumet Specialty Products, Indianapolis, IN), and a yellow oil (America's Core 600, ExxonMobil Basestocks, Spring, TX, a processed lube basestock, containing 0.25% S). Strong anion exchange (SAX) solid-phase extraction (SPE) cartridges (Agilent Bond Mega BE-SAX) were used for ketone separation, and Amplifex keto reagent (AB Sciex, Framingham, MA) was purchased for derivatization.

Commercial NAP Acid Preparation. Commercially available naphthenic acids (TCI America, Portland, OR) were diluted with a white mineral oil to prepare a TAN 6.5 solution.

Ohio University Test Protocol. The Ohio University (OU) has developed a protocol for testing the resistance of corrosion scales to further corrosion.[29] In the OU protocol, corrosion with a test oil on metal rings in a sealed autoclave ("pretreatment") is used to develop an iron sulfide (FeS) corrosion scale; these rings are transferred to a flow-through reactor, where the scale on the rings is "challenged" (to determine extent of corrosion protection) with naphthenic acid solution of fixed TAN in a white oil under rotational shear stress. The details of this protocol have been presented elsewhere.[13,14] Briefly,

(1) "Ring pretreatment": carbon steel (A106 Gr B) and 5Cr rings, a mild steel with a content of 5% chromium (F5 (A182)), were pretreated in the static autoclave with a processed lube

basestock ("yellow oil") containing 0.25% S that generated corrosion scales on the ring surface. The pretreatment temperature was 650 °F (343 °C) and the duration was 24 h.

(2) "Ring challenge": after pretreatment in the static autoclave, the rings were transferred into a high velocity rig (HVR) flow-through reactor, which was fed with the challenge solution of TCI acid in mineral oil (TAN = 6.5, S = <0.1% wt). A schematic diagram of the HVR setup can be seen in Figure S1. The challenge temperature was 650 °F (343 °C) and the duration was 24 h. During the challenge, the speed of the rotating cylinder was set to 2000 rpm (translating to a peripheral velocity of 8.5 m/s, Reynolds number of 1771, and wall shear stress of 74 Pa). A back-pressure of 150 psig was applied to suppress breakout of gas; flow-through rate of fresh oil containing TAN 6.5 TCI acid was set to 7.5 cm^3/min. In addition to the high TAN value of the challenge solution, the high peripheral velocity helped to create a corrosive condition. The solution flowed continuously past the rotating rings at 343 °C with a ~30 min residence time in the HVR. The effluent of the HVR was cooled to room temperature in-line before sampling. Aliquots of effluent were collected in vials at the waste drum hourly during the corrosion test.

All corrosion tests were performed at Ohio University—Institute for Corrosion and Multiphase Technology (ICMT), where the oil samples were collected.

Ketone Separation and Derivatization. Ketones were isolated from post-NAP challenge samples by SAX separation.[28] Briefly, ~1 g aliquot of the sample in the 6th h vial was diluted in 2 mL of pentane and loaded onto a DCM-pretreated SAX SPE cartridge (Agilent Bond Mega BE-SAX) and allowed to equilibrate for 15 min. Fractions were collected by successive 12 mL washes of pentane, DCM, and methanol (MeOH). The solvent in the fractions was evaporated under N_2 and weighed to determine mass balance. The residues were then dissolved in toluene to form 1 mg/mL stock solutions. An aliquot (200 μL) of the stock toluene solution of the DCM fraction was derivatized with Amplifex keto reagent as previously described.[30] As previously shown, the ketones elute in the DCM fraction; hence, only the DCM fraction results are reported.[28]

FT-ICR MS Sample Preparation. The stock toluene solutions of the derivatized DCM fractions from the NAP postchallenge sample were diluted to a final concentration of 250 μg/mL in toluene/methanol (50:50, v/v) without any modifier to aid in protonation. A syringe pump (500 nL/min flow rate) delivered the samples to the mass spectrometer through a 50 μm inner diameter fused silica micro electrospray ionization (ESI) needle under typical positive ESI conditions (i.e., 3.0 kV with a heated metal capillary temperature of ~100 °C). For characterization of the commercial NAP carboxylic acids, the samples were delivered to the mass spectrometer under typical negative ESI conditions with no changes in sample composition.

FT-ICR MS Mass Analysis. A custom-built passively shielded 9.4 T FT-ICR mass spectrometer[31] was equipped with a modular software package (Predator) for data acquisition.[32] Ions generated at atmospheric pressure under the aforementioned ESI conditions were transferred by a tube lens/skimmer at 250 V into an radio frequency (rf)-only external quadrupole. After ion accumulation,[33] the ions were passed through a mass-resolving rf-only quadrupole and collisionally cooled with He gas at a pressure of ~3.5 × 10^{-6} Torr. Octopole ion guides, equipped with capacitively coupled excitation electrodes, transferred the ions into a seven-segment cylindrical ICR cell,[34,35] where they were subjected to broadband frequency sweep excitation (~70−720 kHz at a sweep rate of 50 Hz/μs and peak-to-peak amplitude, $V_{p-p°}$, of 0.57 V). Then, 150 time-domain transients were coadded,[36] zero-filled, fast Fourier transformed, and phase-corrected to yield an absorption-mode mass spectrum for each sample.[37]

FT-ICR MS Mass Calibration and Data Analysis. The mass spectrometer was initially externally calibrated with HP mix (Agilent, Santa Clara, CA) to convert the ICR frequencies to m/z based on a quadrupolar trapping potential approximation.[38,39] From peaks with a

magnitude at least 6 times greater than the standard deviation of the baseline noise, peak lists were constructed. From the peak lists, the spectra were subjected to an internal "walking" calibration,[36] based on the most abundant homologous ion series. The ion masses were converted to the Kendrick mass scale, assigned a unique elemental (containing less than 100 ^{12}C, 200 ^{1}H, 2 ^{14}N, 5 ^{16}O, and 1 ^{32}S atoms and their isotopes), and grouped by heteroatom class ($O_oN_nS_s$) with differing extents of alkylation.[40] Custom software was used for all data processing and imaging (PetroOrg).[41]

Calculated O_1 Distribution Generation. An O_1 distribution was generated based on the O_2 molecular formulas assigned in (−) ESI for the commercial NAP acids. That is, all possible combinations of two acids (assigned O_2 molecular formulas) were used to form a set of O_1 species based on reaction 4. Abundance of the O_1 species was adjusted based on the peak magnitude of the two O_2 assignments to generate a statistical (calculated) distribution of O_1 ketones.

■ RESULTS AND DISCUSSION

Acid Molecular Composition. The molecular composition of the (−) ESI O_2 class (e.g., carboxylic acids) of the commercial NAP used for the open system corrosion test is displayed in Figure 1 (left). Here, isoabundance-contoured
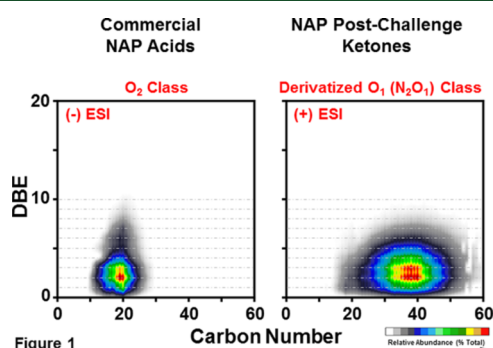
Figure 1. Isoabundance-contoured DBE versus carbon number plots for members of the O_2 class (carboxylic acids) of the commercial NAP acids, based on (−) ESI FT-ICR MS (left) and of the derivatized O_1 (N_2O_1) class from the DCM fraction of the NAP postchallenge sample based on (+) ESI FT-ICR MS (right). The acids have a carbon number centered around C_{19-20} and most abundant DBE of 2. The derivatized ketones/aldehydes have a carbon number range of $\sim C_{25-50}$, with the most abundant at DBE ≈ 2−3.

plots of double bond equivalents (DBE = number of rings plus double bonds to carbon) versus number of carbon atoms enable visualization of the compositional distribution of members of the O_2 heteroatom class. The naphthenic acids are centered at $\sim C_{20}$ and DBE 2 (i.e., one cycloalkane ring plus the carboxyl group). That distribution is typical of commercial NAPs generally derived from lighter, lower boiling point, fractions (e.g., diesel/light gas oil fractions).[42]

Class Distributions Derived from FT-ICR MS Analysis. DCM fractions of the NAP postchallenge effluent samples after SAX separation, along with a sample of the commercial NAP acids, were derivatized and analyzed by (+) ESI FT-ICR MS to characterize any ketone formation. The relative abundances of the assigned heteroatom classes are highlighted in Figure 2. We previously demonstrated the lack of ketones/aldehydes in the white oil used for acid dilution.[28] No assignments were made for the commercial NAP acid mixture, indicating that commercial mixture contained no ketones/aldehydes. In the DCM fraction of the NAP posttest sample, approximately 45% of the relative abundance is assigned to the N_2O_1 class, corresponding to derivatized O_1 ketones/aldehydes. Additional
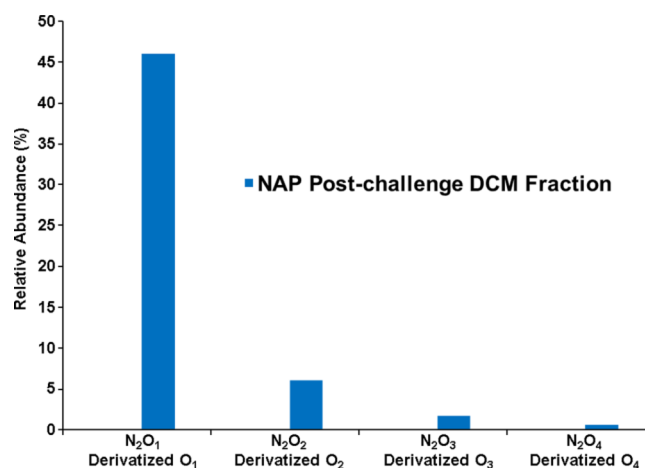
Figure 2. Heteroatom class distributions based on assignments made for derivatized commercial NAP acids (red) and the DCM fraction of the NAP postchallenge sample (blue) based on (+) ESI FT-ICR MS. No peaks were assigned for the commercial NAP, indicating a lack of ketones or aldehydes in the mixture. Most ($\sim$45%) of the relative abundance of the posttest sample was assigned as N_2O_1, corresponding to derivatized ketones/aldehydes generated as a result of the corrosion test.

higher oxygen (i.e., O_2, O_3, and O_4) classes were also derivatized, albeit at decreasingly lower abundances. With such high relative abundances of derivatized O_1 species after the corrosion test, and the absence of any assigned in the pretest, it is clear that ketones/aldehydes were generated as a result of the corrosion test. As noted above, the residence period of the challenge fluid in the autoclave, exposed to the metal rings, is $\sim$30 min. The assignment of ketones in the posttest fluid is consistent with a high corrosion rate at the test temperature (343 °C) and the formation of an iron oxide scale on the metal surfaces. In tests at lower acid concentration, it has been demonstrated that an oxide layer is formed under a pre-existing scale, and a similar layer was formed in the current corrosion test (not shown).[11−14] As noted above, iron naphthenates in solution decompose at lower temperature than the acids; hence, it is postulated that the formation of the ketones and magnetite occurs in solution beneath the porous FeS scale. That is, the ketones represent the acid structures that formed them.

Ketone Molecular Characterization. The molecular composition of the derivatized O_1 class (N_2O_1) of the post-corrosion test sample is displayed in Figure 1 (right). The composition has been adjusted to remove the carbons from the derivatization reagent, displaying only carbons from the reactive ketone/aldehyde. The reagent has no effect on detected DBE. In the thermal decomposition of iron carboxylates, a ketone roughly double in carbon number of the reactive acids and with a DBE one less than the sum of the acid's DBE is expected to be generated (reaction 4). The derivatized O_1 class distribution in the postchallenge fluid exhibits carbon numbers ranging from $\sim C_{25}-C_{50}$, centered around $\sim C_{35}-C_{41}$, and the most abundant DBE ≈ 2−3. Thus, the ketone distribution falls in the range of carbon number and DBE expected for the acids used. The centering of the ketones at $\sim C_{35}-C_{41}$ is consistent with reactive acids of carbon numbers roughly $C_{17}-C_{21}$, corresponding to the most abundant acids in the commercial NAP mixture. The high abundance of ketones at DBE 2 and the detection of DBE 1

ketones suggest a low DBE bias for the commercial naphthenic acids reacting with the iron. The DBE 2 ketones can form only as a result of alkyl carboxylic acids (DBE 1) pairing in reaction 1 with the DBE 2 acids detected with high abundance in the commercial mixture (Figure 1, left). DBE 1 ketones can form only from pairing of two alkyl carboxylic acids. The DBE 3 ketones also observed at high abundance may form as a result of an alkyl carboxylic acid pairing with a DBE 3 acid or two DBE 2 acids pairing together.

Comparison with Calculated Ketone Distributions. Because the mechanisms for iron carboxylate formation (reaction 1) and decomposition (reaction 4) are known along with the initial (unreacted) distribution of the carboxylic acids, we are able to calculate a ketone distribution for the NAP acids, assuming no bias with respect to carbon number or DBE. The ketone distribution calculated from the NAP acids (Figure 3, top right) exhibits a carbon number range of $\sim C_{28}-$
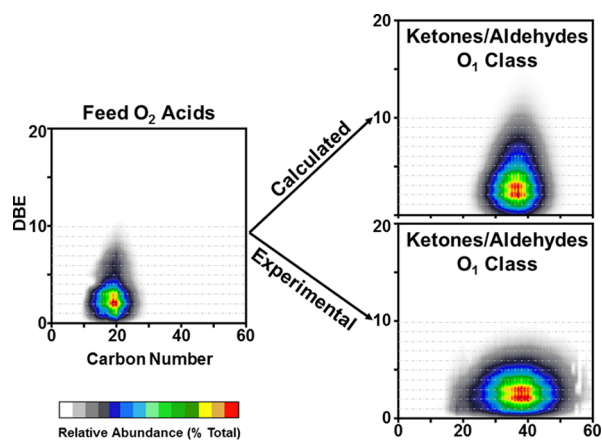
Figure 3. Calculated versus experimental isoabundance-contoured DBE versus carbon number plots for ketones generated by the naphthenic acids based upon the commercial NAP O_2 class distribution. The calculated ketone distribution has a carbon number range of $\sim C_{28}-C_{45}$ and most abundant at DBE $\approx$ 2−3: closely matching the experimental results and indicating a high probability that the ketones were generated by means of an iron carboxylate decomposition mechanism.

C_{45} and most abundant DBEs of 2 and 3. The center of the experimental distribution (Figure 3, bottom left) closely matches the calculated distribution, indicating that the iron carboxylate decomposition mechanism likely plays a strong role in the ketone generation. The experimental results display a wider carbon number range, likely an artifact of the abundance-weighting in the calculation. Upon close examinations, the derivatization reveals that some lower and higher carbon number ketones/aldehydes may be present at very low abundance. The calculation in the model predicts that some ketones at $\sim C_{31}-C_{42}$ could be generated from the higher DBE (possibly aromatic) acids centered at $\sim C_{19}$. No such ions are detected in the experimental results, suggesting that they do not react with the iron, or that their iron salts do not form ketones under the present experimental reaction conditions. The close match between the calculated and experimental distributions demonstrates the potential of the separation/ derivatization method to quantify ketone distributions from mixtures of acids. However, little selectivity among ketones has been detected in the narrow distribution of acid structures for commercial naphthenic acids.

■ ASSOCIATED CONTENT

Ⓢ Supporting Information

The Supporting Information is available free of charge on the ACS Publications website at DOI: 10.1021/acs.energy-fuels.9b00626.

Schematic representation of the HVR flow-through reactor (PDF)

■ AUTHOR INFORMATION

Corresponding Author

*E-mail: marshall@magnet.fsu.edu. Phone: +1 850-644-0529. Fax: +1 850-644-0133.

ORCID Ⓞ

Alan G. Marshall: 0000-0001-9375-2532
Ryan P. Rodgers: 0000-0003-1302-2850

Notes

The authors declare no competing financial interest.

■ REFERENCES

(1) Kapusta, S. D.; Ooms, A.; Smith, A.; Fort, W. C. *Safe Processing of High Acid Crudes*; NACE International, 2004.

(2) Asrar, N.; MacKay, B.; Birketveit, Ø.; Stopanicev, M.; Jackson, J. E.; Jenkins, A.; Melot, D.; Scheie, J.; Vittonato, J. Corrosion—The Longest War. *Oilfield Rev.* **2016**, *28*, 34−49.

(3) Slavcheva, E.; Shone, B.; Turnbull, A. Review of naphthenic acid corrosion in oilrefining. *Br. Corros. J.* **1999**, *34*, 125−131.

(4) Babaian-Kibala, E.; Craig, H. L., Jr.; Rusk, G. L.; Blanchard, K. V.; Rose, T.; Uehlein, B. L.; Quinter, R.; Summers, M. A. Naphthenic Acid Corrosion in Refinery Settings. *Mater. Perform.* **1993**, *32*, 50−55.

(5) Huang, B. S.; Yin, W. F.; Sang, D. H.; Jiang, Z. Y. Synergy Effect of Naphthenic Acid Corrosion and Sulfur Corrosion in Crude Oil Distillation Unit. *Appl. Surf. Sci.* **2012**, *259*, 664−670.

(6) Qu, D. R.; Zheng, Y. G.; Jing, H. M.; Yao, Z. M.; Ke, W. High Temperature Naphthenic Acid Corrosion and Sulphidic Corrosion of Q235 and 5Cr1/2Mo Steels in Synthetic Refining Media. *Corros. Sci.* **2006**, *48*, 1960−1985.

(7) Rebak, R. B. Sulfidic Corrosion in Refineries - A Review. *Corros. Rev.* **2011**, *29*, 123−133.

(8) Laredo, G. C.; López, C. R.; Álvarez, R. E.; Castillo, J. J.; Cano, J. L. Identification of Naphthenic Acids and Other Corrosivity-Related Characteristics in Crude Oil and Vacuum Gas Oils from a Mexican Refinery. *Energy Fuels* **2004**, *18*, 1687−1694.

(9) Smart, N. R.; Rance, A. P.; Pritchard, A. M. *Laboratory Investigation of Naphthenic Acid Corrosion under Flowing Conditions*; NACE International, 2002.

(10) El Kamel, M.; Galtayries, A.; Vermaut, P.; Albinet, B.; Foulonneau, G.; Roumeau, X.; Roncin, B.; Marcus, P. Sulfidation kinetics of industrial steels in a refinery crude oil at 300 °C: reactivity at the nanometer scale. *Surf. Interface Anal.* **2010**, *42*, 605−609.

(11) Jin, P.; Robbins, W.; Bota, G. Mechanism of High Temperature Corrosion by Model Naphthenic Acids. *NACE Corrosion*, 2016; p 7302.

(12) Jin, P.; Nesic, S.; Wolf, H. A. Analysis of Corrosion Scales Formed on Steel at High Temperatures in Hydrocarbons Containing Model Naphthenic Acids and Sulfur Compounds. *Surf. Interface Anal.* **2015**, *47*, 454−465.

(13) Jin, P.; Bota, G.; Robbins, W.; Nesic, S. Analysis of Oxide Scales Formed in the Naphthenic Acid Corrosion of Carbon Steel. *Energy Fuels* **2016**, *30*, 6853−6862.

(14) Jin, P.; Robbins, W.; Bota, G. Mechanism of Magnetite Formation in High Temperature Corrosion by Model Naphthenic Acids. *Corros. Sci.* **2016**, *111*, 822−834.

(15) Yépez, O. On the Chemical Reaction between Carboxylic Acids and Iron, Including the Special Case of Naphthenic Acid. *Fuel* **2007**, *86*, 1162−1168.

(16) Chen, C.-J.; Chiang, R.-K.; Lai, H.-Y.; Lin, C.-R. Characterization of Monodisperse Wüstite Nanoparticles following Partial Oxidation. *J. Phys. Chem. C* **2010**, *114*, 4258−4263.

(17) Salih, K. S. M.; Mamone, P.; Dörr, G.; Bauer, T. O.; Brodyanski, A.; Wagner, C.; Kopnarski, M.; Klupp Taylor, R. N.; Demeshko, S.; Meyer, F.; et al. Facile Synthesis of Monodisperse Maghemite and Ferrite Nanocrystals from Metal Powder and Octanoic Acid. *Chem. Mater.* **2013**, *25*, 1430−1435.

(18) Meredith, W.; Kelland, S.-J.; Jones, D. M. Influence of Biodegradation on Crude Oil Acidity and Carboxylic Acid Composition. *Org. Geochem.* **2000**, *31*, 1059−1073.

(19) Koike, L.; Rebouças, L. M. C.; Reis, F. d. A. M.; Marsaioli, A. J.; Richnow, H. H.; Michaelis, W. Naphthenic Acids from Crude Oils of Campos Basin. *Org. Geochem.* **1992**, *18*, 851−860.

(20) Lalli, P. M.; Corilo, Y. E.; Rowland, S. M.; Marshall, A. G.; Rodgers, R. P. Isomeric Separation and Structural Characterization of Acids in Petroleum by Ion Mobility Mass Spectrometry. *Energy Fuels* **2015**, *29*, 3626−3633.

(21) Hughey, C. A.; Minardi, C. S.; Galasso-Roth, S. A.; Paspalof, G. B.; Mapolelo, M. M.; Rodgers, R. P.; Marshall, A. G.; Ruderman, D. L. Naphthenic Acids as Indicators of Crude Oil Biodegradation in Soil, Based on Semi-Quantitative Electrospray Ionization Fourier Transform Ion Cyclotron Resonance Mass Spectrometry. *Rapid Commun. Mass Spectrom.* **2008**, *22*, 3968−3976.

(22) Hsu, C. S.; Dechert, G. J.; Robbins, W. K.; Fukuda, E. K. Naphthenic Acids in Crude Oils Characterized by Mass Spectrometry. *Energy Fuels* **2000**, *14*, 217−223.

(23) Schempp, P.; Preuß, K.; Tröger, M. About the Correlation Between Crude Oil Corrosiveness and Results From Corrosion Monitoring in an Oil Refinery. *Corrosion* **2016**, *72*, 843−855.

(24) Sekine, I.; Okano, C. Corrosion Behavior of Mild Steel and Ferritic Stainless Steels in Oxalic Acid Solution. *Corrosion* **1989**, *45*, 924−932.

(25) Groysman, A.; Brodsky, N.; Pener, J.; Shmulevich, D. *Low Temperature Naphthenic Acid Corrosion Study*; NACE International, 2007.

(26) Kane, R. D.; Chambers, B. High Temperature Crude Oil Corrosivity: Where Sulfur and Naphthenic Acid Chemistry and Metallurgy Meet. *Corrosion Solutions Conference*, Lake Louise, Alberta, Canada, 2011.

(27) Messer, B.; Beaton, M. C.; Tarleton, B.; Phillips, T. T. *New Theory for Naphthenic Acid Corrosivity of Athabasca Oilsands Crudes*; NACE International, 2004.

(28) Krajewski, L. C.; Lobodin, V. V.; Robbins, W. K.; Jin, P.; Bota, G.; Marshall, A. G.; Rodgers, R. P. Method for Isolation and Detection of Ketones Formed from High-Temperature Naphthenic Acid Corrosion. *Energy Fuels* **2017**, *31*, 10674−10679.

(29) Wolf, H. A.; Cao, F.; Blum, S. C.; Schilowitz, A. M.; Ling, S.; McLaughlin, J. E.; Nesic, S.; Jin, P.; Bota, G. Method for Identifying Layers Providing Corrosion Protection in Crude Oil Fractions. U.S. Patent 9,140,640, 2015.

(30) Alhassan, A.; Andersson, J. T. Ketones in Fossil Materials-A Mass Spectrometric Analysis of a Crude Oil and a Coal Tar. *Energy Fuels* **2013**, *27*, 5770−5778.

(31) Kaiser, N. K.; Quinn, J. P.; Blakney, G. T.; Hendrickson, C. L.; Marshall, A. G. A Novel 9.4 Tesla FTICR Mass Spectrometer with Improved Sensitivity, Mass Resolution, and Mass Range. *J. Am. Soc. Mass Spectrom.* **2011**, *22*, 1343−1351.

(32) Blakney, G. T.; Hendrickson, C. L.; Marshall, A. G. Predator Data Station: A Fast Data Acquisition System for Advanced FT-ICR MS Experiments. *Int. J. Mass Spectrom.* **2011**, *306*, 246−252.

(33) Senko, M. W.; Hendrickson, C. L.; Emmett, M. R.; Shi, S. D. H.; Marshall, A. G. External Accumulation of Ions for Enhanced Electrospray Ionization Fourier Transform Ion Cyclotron Resonance Mass Spectrometry. *J. Am. Soc. Mass Spectrom.* **1997**, *8*, 970−976.

(34) Kaiser, N. K.; Savory, J. J.; McKenna, A. M.; Quinn, J. P.; Hendrickson, C. L.; Marshall, A. G. Electrically Compensated Fourier Transform Ion Cyclotron Resonance Cell for Complex Mixture Mass Analysis. *Anal. Chem.* **2011**, *83*, 6907−6910.

(35) Tolmachev, A. V.; Robinson, E. W.; Wu, S.; Kang, H.; Lourette, N. M.; Paša-Tolić, L.; Smith, R. D. Trapped-Ion Cell with Improved DC Potential Harmonicity for FT-ICR MS. *J. Am. Soc. Mass Spectrom.* **2008**, *19*, 586−597.

(36) Savory, J. J.; Kaiser, N. K.; McKenna, A. M.; Xian, F.; Blakney, G. T.; Rodgers, R. P.; Hendrickson, C. L.; Marshall, A. G. Parts-Per-Billion Fourier Transform Ion Cyclotron Resonance Mass Measurement Accuracy with a "Walking" Calibration Equation. *Anal. Chem.* **2011**, *83*, 1732−1736.

(37) Xian, F.; Hendrickson, C. L.; Blakney, G. T.; Beu, S. C.; Marshall, A. G. Automated Broadband Phase Correction of Fourier Transform Ion Cyclotron Resonance Mass Spectra. *Anal. Chem.* **2010**, *82*, 8807−8812.

(38) Ledford, E. B.; Rempel, D. L.; Gross, M. L. Space Charge Effects in Fourier Transform Mass Spectrometry. II. Mass Calibration. *Anal. Chem.* **1984**, *56*, 2744−2748.

(39) Shi, S. D.-H.; Drader, J. J.; Freitas, M. A.; Hendrickson, C. L.; Marshall, A. G. Comparison and Interconversion of the Two Most Common Frequency-to-Mass Calibration Functions for Fourier Transform Ion Cyclotron Resonance Mass Spectrometry. *Int. J. Mass Spectrom.* **2000**, *195−196*, 591−598.

(40) Hughey, C. A.; Hendrickson, C. L.; Rodgers, R. P.; Marshall, A. G.; Qian, K. Kendrick Mass Defect Spectrum: A Compact Visual Analysis for Ultrahigh-Resolution Broadband Mass Spectra. *Anal. Chem.* **2001**, *73*, 4676−4681.

(41) *PetroOrg*; The Florida State University, All Rights Reserved, 2017.

(42) Brient, J. A.; Wessner, P. J.; Doyle, M. N. Naphthenic Acids. *Kirk−Othmer Encyclopedia of Chemical Technology*; John Wiley & Sons, Inc.: Hoboken, NJ, USA, 2000.